

## Article

# Assessment of Future Water Security under Climate Change: Practical Water Allocation Scenarios in a Drought-Prone Watershed in South Korea

Wonjin Kim, Sijung Choi \*, Seongkyu Kang  and Soyoung Woo 

Department of Hydro Science and Engineering Research, Korea Institute of Civil Engineering and Building Technology, Goyang 411-712, Republic of Korea; wjkim@kict.re.kr (W.K.); skkang@kict.re.kr (S.K.); wsy0209@kict.re.kr (S.W.)

\* Correspondence: sjchoi@kict.re.kr

**Abstract:** Seomijn River Basin has numerous hydraulic structures designed to satisfy water demands and mitigate future droughts. However, the increasing water demand and export to neighboring areas cause water deficits and conflicts between water users. Therefore, practical strategies to mitigate the potential damage from climate change are essential. In this study, we aimed to propose practical strategies under climate change by examining the future water security of the Seomjin River Basin under five different water allocation scenarios referenced from the practical policies of various countries. Future climate models determined based on extreme precipitation indices of the ETCCDI were used to investigate their impact on water security, which was evaluated using unmet demand; demand coverage; reliability, resilience, and vulnerability; and aggregation index metrics. We found that prioritizing domestic and industrial water use is the optimal water security strategy, and unconditional allocation of instream flow can cause a significant water deficit for other water uses. However, prioritizing all water uses equally also proved effective under some conditions. Thus, our study highlights the importance of adaptive management and suggests that the optimal water allocation strategy lies in its flexibility in response to varying circumstances.

**Keywords:** climate change; drought; water security; water allocation



**Citation:** Kim, W.; Choi, S.; Kang, S.; Woo, S. Assessment of Future Water Security under Climate Change: Practical Water Allocation Scenarios in a Drought-Prone Watershed in South Korea. *Water* **2024**, *16*, 2933. <https://doi.org/10.3390/w16202933>

Academic Editor: Yaning Chen

Received: 13 August 2024

Revised: 6 October 2024

Accepted: 12 October 2024

Published: 15 October 2024



**Copyright:** © 2024 by the authors. Licensee MDPI, Basel, Switzerland. This article is an open access article distributed under the terms and conditions of the Creative Commons Attribution (CC BY) license (<https://creativecommons.org/licenses/by/4.0/>).

## 1. Introduction

Climate change, or climate crisis, is a severe and urgent issue. Since the 18th century industrial revolution and the rapid rise in carbon dioxide emissions post-1970s, environmental changes and natural disasters have increased dramatically [1,2]. Although the frequency of geophysical disasters such as earthquakes and volcanoes has remained relatively stable over the past decades, the frequency of climate and hydrological disasters such as droughts and floods has increased, directly threatening human survival and prosperity. Anthropogenic influences have already affected weather and extreme climate events worldwide [3]. Changes in hydrometeorological phenomena owing to recent climate change have led to increased damage from extreme floods and droughts. Since the 1970s, the variance in annual precipitation has increased, leading to severe droughts every five to seven years. The number of drought days surged to an average of 63.1 days in the 2010s, indicating a rising trend in drought occurrence. Projections suggest that the average precipitation will increase by up to 16.0% by the latter half of the 21st century, whereas the number of rainy days will decrease. Climate change is the most significant risk factor in water resource management, highlighting the urgent need for proactive water disaster response strategies [4,5].

Drought, characterized by prolonged periods of deficient rainfall, is a slow-onset natural disaster that causes significant economic, social, and environmental disruptions, making it the most expensive climate-related disaster worldwide [6,7]. The term drought can be distinguished from the perspectives of natural events and risk factors. As a natural event,

drought typically refers to a temporary shortage of precipitation below the normal levels for a specific watershed [8]. In contrast, from a risk perspective, drought signifies a scenario in which reduced precipitation leads to water resources failing to meet the demand, resulting in water scarcity [9]. Water scarcity due to drought is one of the most severe risks faced by water resource managers, who have traditionally designed water resource management systems to maintain water supply during the worst droughts [10]. With the increasing frequency and duration of droughts due to human activity and climate change [11–13], understanding the vulnerability of hydrological cycles and drought conditions is crucial. This underscores the need for robust management plans to address possible dry scenarios.

Increases in urban and industrial water demand and growing concerns regarding environmental flow must be addressed from the perspectives of sustainable development, social balance, and equity. Therefore, water security, which defines the societal needs for water and resilient ecosystems, is a key concept for evaluating water infrastructure, allocation, and management at different watershed scales [14]. Although the importance of water security is expected to intensify in the future and become more vulnerable, the expanding quantitative water supply through hydraulic structures is becoming increasingly constrained owing to economic and environmental reasons within a limited territory. Therefore, traditional water management policies, such as water supply enhancement in regional dimensions, should be replaced by sustainable policies that constitute the core of sustainable development, as defined by the World Commission on Environment and Development, to ensure the needs of the present without compromising on the future generations' ability to meet their needs [15–17].

Allocation regimes typically follow a predetermined sequence of priorities. These regimes manage priority access to water during competition, under normal conditions or exceptional circumstances, such as scarcity and drought. In many countries, allocation regimes prioritize water use for domestic, human, and national needs. However, there are exceptions such as the Netherlands, some Canadian Provinces, Israel, and Peru. For example, in the Netherlands, the highest priorities are safety (preventing dike collapse) and environmental damage prevention. The second most common priority is agriculture or environmental use. Allocation regimes of some countries specify priority uses in great detail, with Hungary, Mexico, and Peru having six distinct levels and Spain and South Africa having five distinct levels [18]. The different priority sequences defined in various allocation regimes are illustrated in Figure 1. These diverse implementations demonstrate a wide range of water allocation practices. In South Korea, the allocation sequence prioritizes domestic and industrial use, followed by agricultural use and environmental flow maintenance. However, this allocation system faces challenges, particularly during periods of prolonged drought or increased water demand, and more flexible management strategies are needed to ensure that all essential water requirements are met without compromising long-term sustainability. Improved infrastructure operations, better water conservation practices, and enhanced regulatory frameworks should be considered to comprehensively overcome these challenges.

Much research has been performed on water security and allocation. In South Korea, Lee et al. [19] proposed a decision-making method for prioritizing water allocation during droughts using an analytic hierarchy process (AHP) method. Choi et al. [20] prioritized different scenarios for water budget analysis using multi-criteria decision analysis. Lim et al. [21] determined the standard level of reservoir storage under different priority scenarios for domestic, industrial, and agricultural water use and assessed the degree of water scarcity to evaluate the contribution of dams in maintaining ecological flow. Kim et al. [22] proposed an efficient approach for evaluating the risks of system failures within a decision-centric framework based on a water allocation model. Internationally, Wang et al. [23] optimized the operating rules for a reservoir system to account for ecological flow and water use priorities, whereas Luo et al. [24] provided a comprehensive overview of water management policies based on water use priorities. Zehtabian et al. [25] considered the appropriate priorities for all demands and applied environmental flow in integrated water resource management to offer practical options for water management.

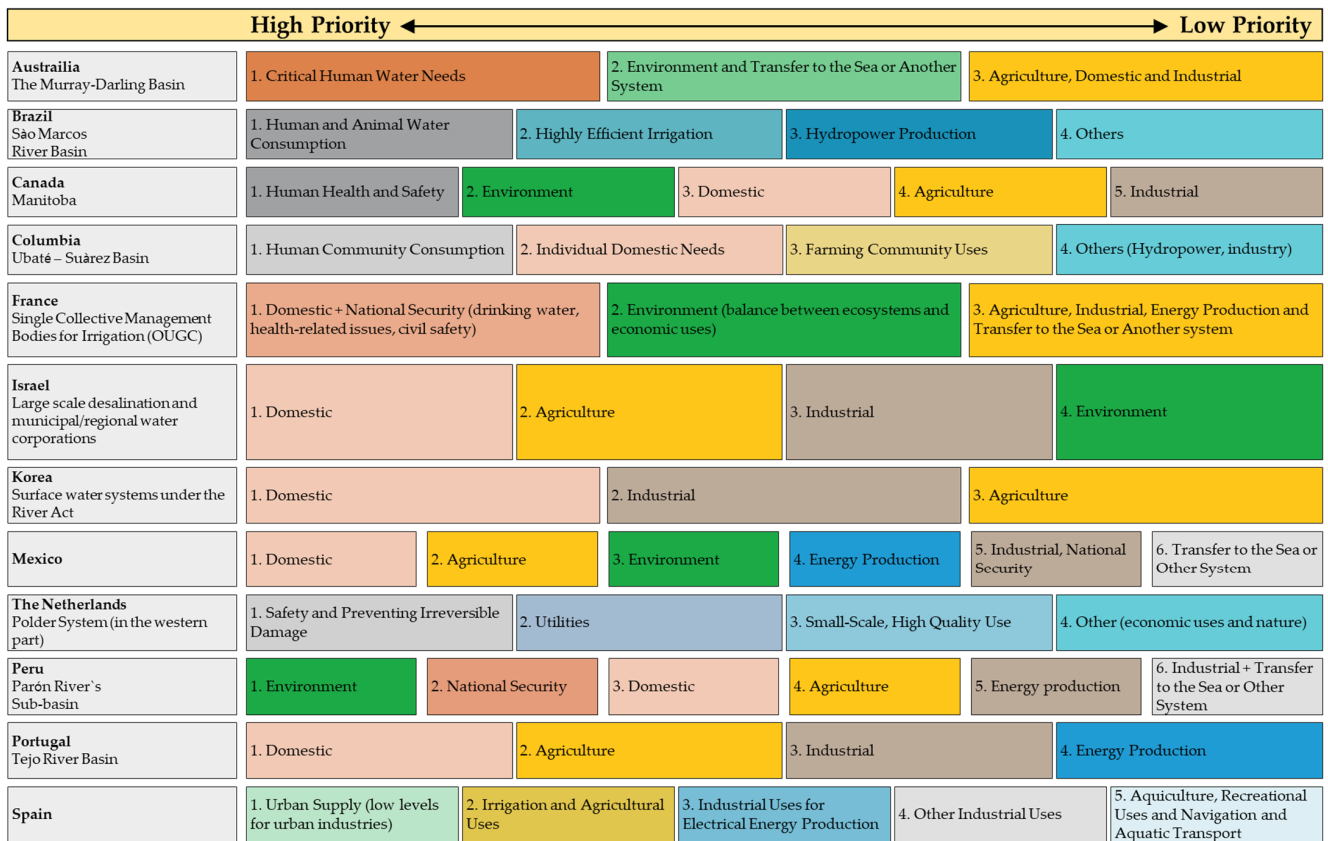


Figure 1. Sequence of water use priority in different countries [18].

Previous studies on water security and allocation have primarily focused on methodologies for optimizing water management systems. However, these studies meet certain limitations in evaluating future water security unless proposing practical policies with quantitative results under various climate conditions. Therefore, this study aimed to evaluate future water security under various climate change scenarios, especially dry scenarios, by applying practical water allocation strategies. Three distinct dry scenarios were selected and five different water allocation strategies were applied to each climate scenario to assess the impact of water allocation on future water security and to provide comprehensive insights into sustainable water resource management during climate change in the Seomjin River Basin.

## 2. Materials and Methods

### 2.1. Study Area

The Seomjin River Basin is situated in southern South Korea and covers an approximate area of 8298 km<sup>2</sup>. The basin is comprised of two major watersheds, Seomjin River and Seomjin River Downstream. Seomjin River Watershed features the Seomjin River, one among the five largest rivers in South Korea. The river originates in the north, and its largest tributary, the Boseong River, originates in the southwest and merges with it. In contrast, Seomjin River Downstream Watershed lacks sufficiently large rivers and drains directly into the sea; however, it hosts significant national industrial complexes. Figure 2 illustrates the study area.

Multiple dams have been constructed in Seomjin River Watershed, where resources for water supply are abundant, to meet the increasing water demand. These include multipurpose dams (the Seomjin and Juam dams), water supply dams (the Dongbok, Donghwa, and Sueo Dams), and hydroelectric dams (the Boseong River dam). However, because of the substantial water demand from adjacent administrative districts and industrial complexes, approximately 80% of the water secured by hydraulic structures is transferred to the outer and inner watersheds. This situation can cause potential conflicts between water users during droughts when the main river flow becomes insufficient. In addition, the estuary of watershed

is the primary site for domestic harvesting, particularly of corbicula (a type of freshwater clam). However, the recent expansion of the Daap intake station's capacity and increased water intake have reduced downstream flow and degraded water quality, damaging corbicula production and leading to complaints from local residents. Thus, despite numerous water storage facilities, the basin remains vulnerable to drought and faces challenges regarding water allocation. Therefore, comprehensive analyses of water security and demand management plans for different watershed scenarios should be considered.

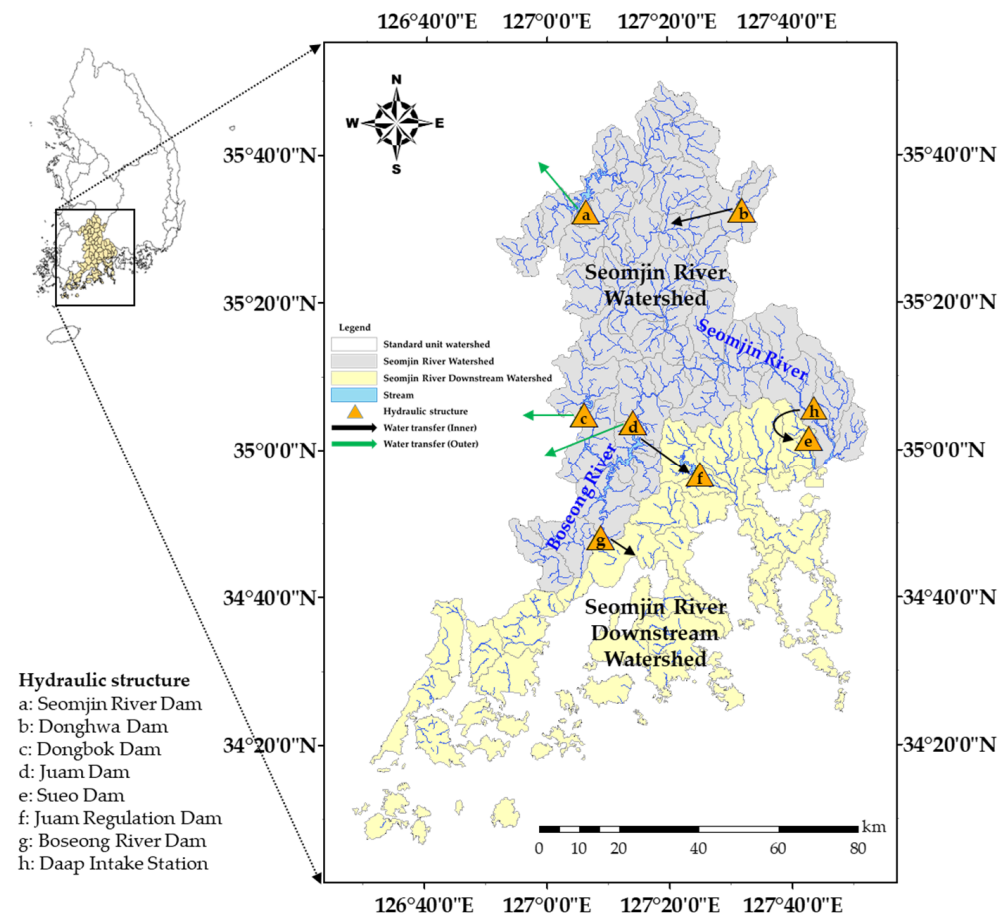


**Figure 2.** Description of study area.

## 2.2. Soil and Water Assessment Tool

Soil and Water Assessment Tool (SWAT) is a physically based, semi-distributed model designed to predict the continuous and long-term hydrological cycle of a watershed under various soil types, land covers, climate conditions, and management practices [26]. Developed by the United States Department of Agriculture, Agricultural Research Service, the model enables the efficient processing and computation of continuous simulations over a long time [27]. Spatially distributed data on land use, topography, and soil are used as inputs (Figure 3) to estimate outputs such as runoff, evapotranspiration, percolation, sediment, and nutrients [28–30]. The hydrological process simulated by SWAT is based on the following balanced equation:

$$SW_t = SW_0 + \sum_{i=1}^t (R_{day} - Q_{surf} - W_{seep} - E_a - Q_{gw}) \quad (1)$$

where  $SW_t$  is the humidity of the soil (mm),  $SW_0$  is the base humidity of the soil (mm),  $t$  is the time (days),  $R_{day}$  is the rainfall volume (mm),  $Q_{surf}$  is the surface runoff,  $E_a$  is the

evapotranspiration (mm),  $W_{seep}$  is the seepage of water from the soil into deeper layers, and  $Q_{gw}$  is the underground runoff (mm).

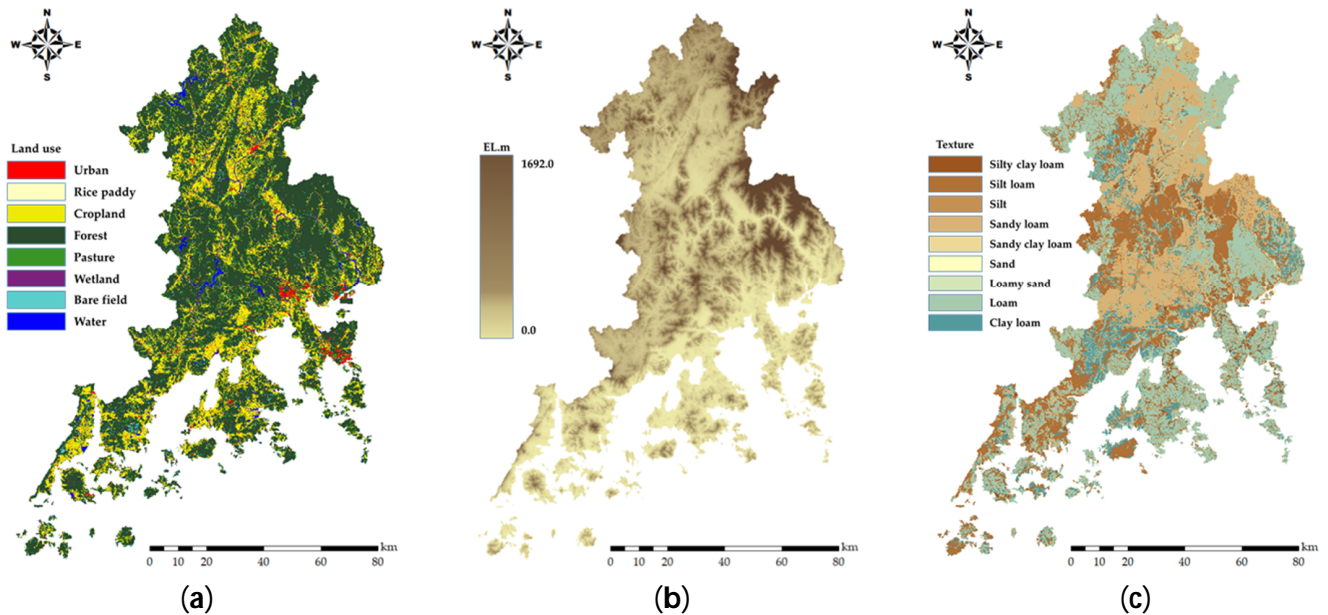


**Figure 3.** SWAT input data: (a) land use map; (b) digital elevation map; (c) soil map.

SWAT was used to estimate and provide natural runoff, and its calibration was performed by excluding observation points located downstream of the hydraulic structures affected by artificial discharges. Calibration results were evaluated using two objective functions: coefficient of determination  $R^2$  and percent BIAS ( $PBIAS$ ), defined as follows:

$$R^2 = \frac{[\sum(O_i - M)(S_i - S)]^2}{\sum(O_i - M)^2 \sum(S_i - S)^2} \quad (2)$$

$$PBIAS = 100 \times \frac{\sum(O_i - S_i)}{\sum O_i} \quad (3)$$

where  $O_i$  is the observed value at time  $i$ ;  $P_i$  is the simulated value at time  $i$ ;  $M$  is the mean of the observed values; and  $S$  is the mean of the simulated values.

To estimate the natural runoff aligned with our research objectives, the target watershed was delineated into standard watershed units. The calibrated model was used to account for the long-term changes in natural runoff in the water balance analysis by applying future climate change scenarios and historical meteorological data.

### 2.3. K-WEAP

We used the Korea-Water Evaluation and Planning System (K-WEAP), a flexible and visible model that helps users to evaluate water resources by setting scenarios based on different input variables, for the analysis. K-WEAP is a devised version of Water Evaluation and Planning (WEAP) tool developed by Korea Institute of Construction Technology (KICT) and Stockholm Environment Institute–Boston Center (SEI-B) to better consider the characteristics of South Korea [31]. The model provides a comprehensive, user-friendly framework for planning and policy analysis, which can be applied for complex water budget analyses and regional water security observation. It can also represent water resource systems by incorporating natural inflows, water use efficiency, dam operation, and supply priority as input data, allowing it to consider various water supply and demand scenarios. Considering these characteristics and the extensive use of K-WEAP in planning and managing water resources in South Korea at different basin scales [32–34], we used K-WEAP to analyze future water security based on practical water allocation priorities.

### 2.3.1. Model Setting

Spatial resolution of water budget analysis differs according to water use. Domestic and industrial water demands are primarily organized at the administrative district level. Accordingly, locally permitted intake for domestic, industrial, and agricultural uses were applied through a network in a standard watershed unit. Temporal resolution was set to 5-day intervals, aligned with the methodology commonly employed in national water resource plans and evaluations [4,35].

Water supply and demand were considered by establishing a water budget network within the study area. The network illustrates water use, consumption, return, and transfer between water sources and demand sites based on schematic elements of K-WEAP, including transmission link, return flow link, wastewater treatment plant, and local supplies.

The water supply sources were categorized into natural inflow (unregulated inflow) and supply from dams, agricultural reservoirs, and groundwater. The specification and operation data of the hydraulic structures were obtained from relevant institutions, and the structures were mapped onto the network based on geographical information. Given the challenge of individually applying over 1000 agricultural reservoirs in the study area, we applied representative reservoirs of each watershed unit to the network, except for those used for nonagricultural purposes. Groundwater nodes were included in the network, based on administrative or standard watershed units.

Regarding water demand, domestic water use involved the process from intake facilities to wastewater treatment facilities based on each administrative district. Industrial water use was distinguished between local uses and those managed by the government in industrial complexes. Conversely, agriculture water use was separated into irrigation and non-irrigation uses at the standard watershed unit, reflecting the complex interconnections with supply sources, including agricultural reservoirs and groundwater. Figure 4 shows the basic network of domestic, industrial, and agricultural water supply and demand applied in this study.

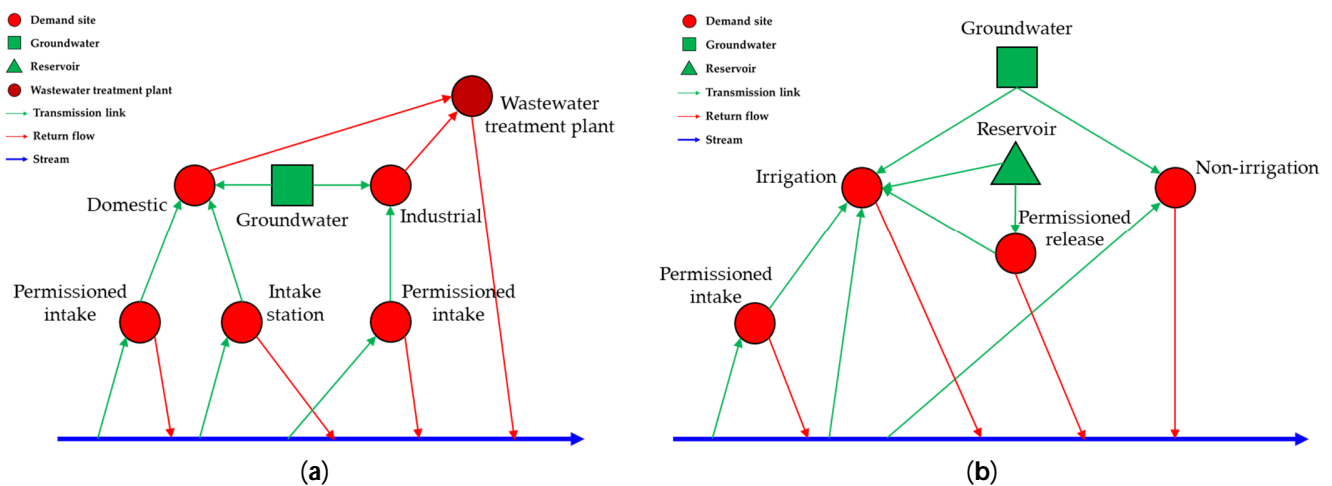


Figure 4. Schematic network of water supply: (a) domestic and industrial supply; (b) agricultural supply.

### 2.3.2. Input Data

Data on unregulated flow, agricultural reservoirs, groundwater resource, and dams serving as supply sources were collected based on data from hydrological models and observed data. The natural runoff simulated by SWAT was assumed to be the total amount of inflow for each sub-watershed, whereas the inflow of representative reservoirs for agricultural purposes within each sub-watershed was determined by considering the ratio of drainage area to watershed area, calculated as follows:

$$Q_{res,i} = Q_{n,i} \times \frac{\sum A_{res,i}}{A_{sub,i}} \tag{4}$$

$$Q_{u,i} = Q_{n,i} - Q_{res,i} \quad (5)$$

where  $A_{res,i}$  is the drainage area of the agricultural reservoir in sub-watershed  $i$ ,  $A_{sub,i}$  is the watershed area of sub-watershed  $i$ ,  $Q_{n,i}$  is the volume of the natural flow of sub-watershed  $i$  estimated by SWAT,  $Q_{res,i}$  is the volume of the inflow of a representative agricultural reservoir in sub-watershed  $i$ , and  $Q_{u,i}$  is the volume of the unregulated flow of sub-watershed  $i$ . The annual recharge of groundwater for each administrative district (domestic and industrial) and a standard watershed unit (agricultural) was estimated by averaging the groundwater use for the corresponding purpose. Moreover, dams within the watershed were considered to release water based on a monthly target release as part of a water supply plan to compensate for unpredictable future releases.

The target water demand, facility capacity, and water consumption were determined to assess future water security. The target water demand was retrieved from the Ministry of the Environment (ME) [4], which recommends the projected water demand by considering population growth, economic development, and agricultural activities. For domestic and industrial water use, water demand was aggregated in the higher administrative division by compiling data from the lower divisions. Data were collected from 11 districts (Imsil, Sunchang, Namwon, Gokseong, Gurye, Hadong, Sunchang, Gwangyang, Boseong, Yeosu, and Goheung) that influence the water resources within the watersheds. The agricultural water demand was organized across 71 standard watershed units. The total amounts of projected water demand for domestic, industrial, and agricultural water use are 118.78 Mm<sup>3</sup>/year, 342.83 Mm<sup>3</sup>/year, and 1044.64 Mm<sup>3</sup>/year, respectively. Figure 5 displays the three types of annual water demand in the target watersheds. Moreover, the capacity of each intake facility was individually considered to account for the currently operating facilities, whereas water consumption during the supply procedure was considered based on the average loss or consumption rate of each demand site to ensure reliability of the water budget analysis.

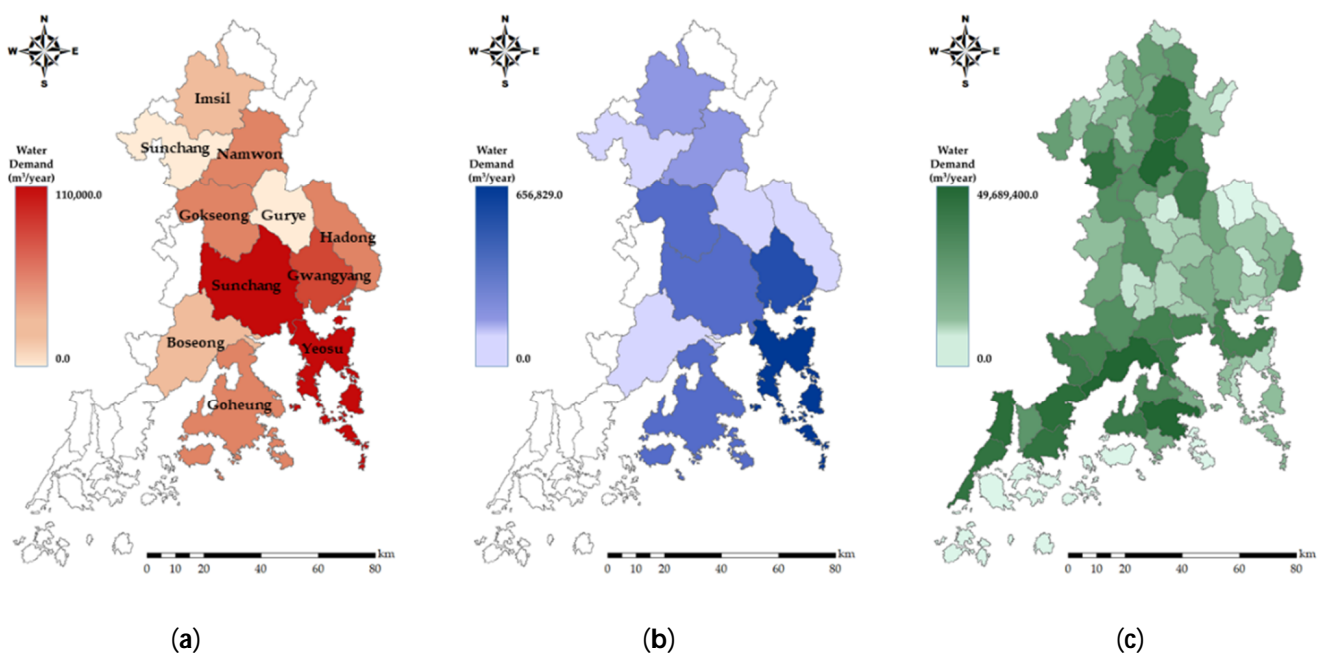


**Figure 5.** Distribution of annual water demand: (a) domestic; (b) industrial; and (c) agricultural demands.

## 2.4. Climate Change Scenarios

### 2.4.1. Coupled Model Intercomparison Project 6

For future climate data, the sixth phase of the coupled model intercomparison project (CMIP6) was used in this study. CMIP6, which is also known as a Shared Socioeconomic Pathways (SSP), considers global economic and demographic changes along with greenhouse gas emissions for climate simulation. Five SSP scenarios (SSP1: sustainability; SSP2: middle of the road; SSP3: regional rivalry; SSP4: inequality; and SSP5: fossil fuel development)

represent different combinations of mitigation and adaptation challenges [36]. Moreover, SSP scenarios are combined with Representative Concentration Pathways (RCPs) using shared policy assumptions to ensure that the future scenarios are reasonable [37,38]. Thus, SSP126 (SSP1-RCP2.6), SSP245 (SSP2-RCP4.5), SSP460 (SSP4-RCP6.0), and SSP585 (SSP5-RCP8.5) are the updated versions of the RCP scenarios from CMIP5. In this study, we employed climate model data obtained from CMIP6 and four SSP scenarios (SSP1–3 and SSP5) over the study area. Table S1 lists 15 general circulation models (GCMs) that are integrated in CMIP6 to satisfy all the necessary input data for the SWAT model, including precipitation, maximum and minimum temperatures, relative humidity, average wind speed, and solar radiation.

#### 2.4.2. Extreme Precipitation Indices

The World Climate Research Program and World Meteorological Organization jointly established the Expert Team on Climate Change Detection and Indices (ETCCDI) to identify the impacts of climate change on extreme water events [39]. The ETCCDI include 27 indices, 11 of which are related to precipitation and 16 to temperature. These indices were calculated based on daily precipitation and temperature values. Notably, frequent natural disasters, such as floods and droughts, in various regions are associated with changes in the frequency and intensity of precipitation extremes. Moreover, the projection of precipitation extremes is a key topic for improving our understanding of the causes and consequences of extreme events on the natural events [40–42]. Therefore, this study relies on the projection of precipitation-related indices among the ETCCDI to understand future changes in climate extremes over the study region. Table S2 presents the definitions of the extreme precipitation indices of the ETCCDI.

#### 2.5. Water Allocation Scenarios

By default, the water allocation priority of each demand site is set to equal in the K-WEAP model, ensuring that all demand sites receive the same satisfaction rate when water resources are insufficient to meet the total demand. However, in reality, the importance of water demand often takes precedence, as different industries exhibit varying tolerances to water shortage. For example, shortage of agricultural water may have minimal societal impact, whereas shortage of domestic water can cause significant societal disruption. Furthermore, differences in development goals, functional positioning, and levels of economic and social development in urban agglomerations necessitate varying water allocation priorities across cities. Therefore, the determination of water allocation should fully consider these factors.

Our water budget analysis employed five scenarios of water allocation priority, as depicted in Figure 6. These scenarios vary in the order of priority given to domestic, industrial, agricultural, and instream flow requirements. The first scenario prioritizes domestic, industrial, and agricultural uses before instream flow. The second scenario gives priority to domestic and industrial needs, followed by agricultural and instream flows. The third scenario considers all uses (domestic, industrial, agricultural, and instream) equally. The fourth and fifth scenarios prioritize instream flow first, with the fourth scenario addressing domestic, industrial, and agricultural needs and the fifth scenario focusing on domestic and industrial uses before agricultural needs. By incorporating these varying priority scenarios, we comprehensively evaluated the impacts of different water allocation strategies on the overall water supply and demand balance.

Figure 7 shows the flow requirement points located within the Seomjin River Basin. Water allocation scenarios were applied to the K-WEAP network by varying the priorities of the demand sites based on their water use purposes. In cases where a dam restricts natural streamflow, different priority criteria were used to allocate water upstream and downstream. There were 13 designated points (Unam-gyo, Iljung-ri, Hyeonpo-ri, Pyeongnam-ri, Yujeok-gyo, Sindeok-ri, Dongrim-gyo, Godal-gyo, Yeseong-gyo, Taeon-gyo, Gurye-gyo, Songjeong-ri, and Gajang-gyo) for instream flow in the target watersheds. All these points were situated within



watershed 40, with one upstream of the Seomjin River Dam, one downstream of the Boseong River Dam, and eleven downstream of the Seomjin River and Juam Dam.

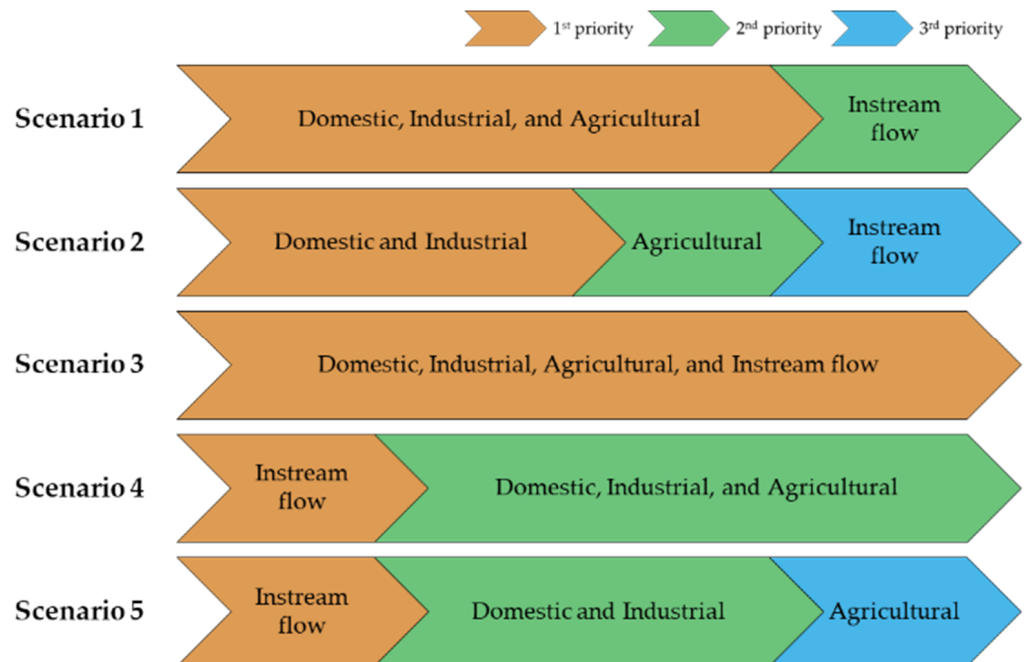


Figure 6. Five water allocation scenarios employed in this study.

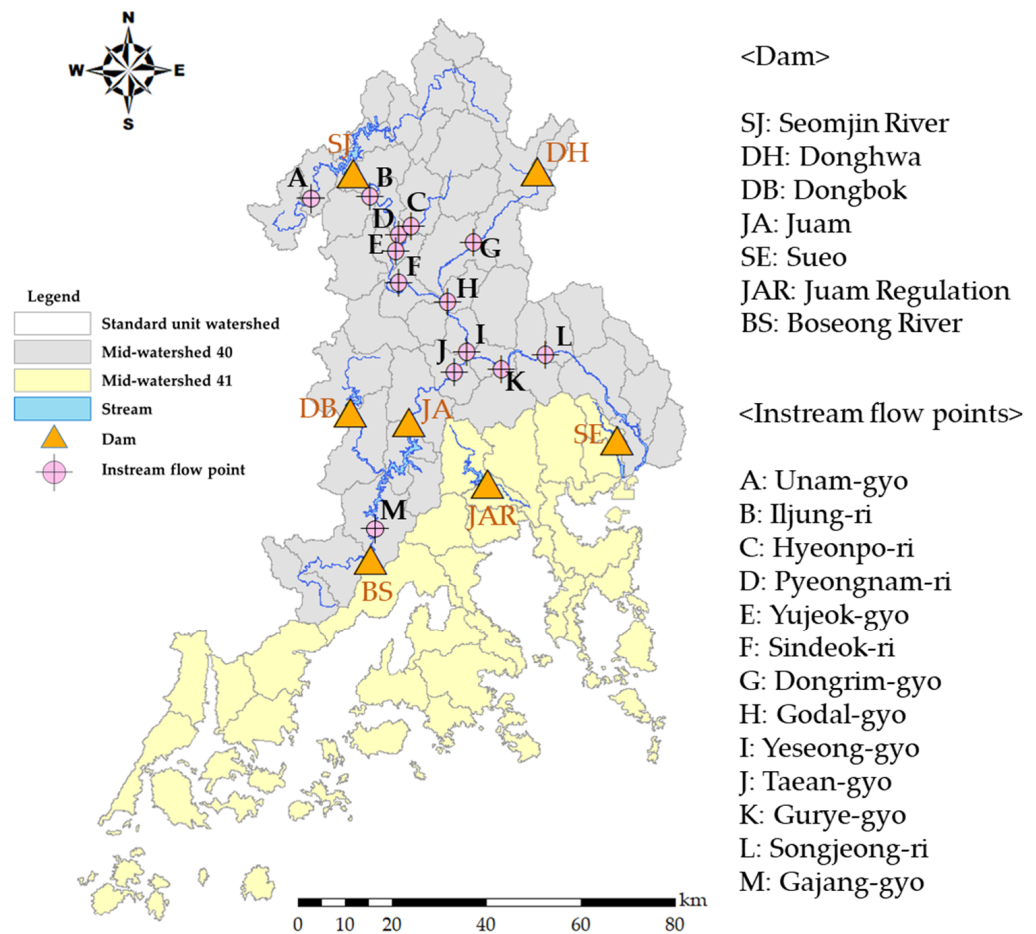


Figure 7. Details of the 13 flow requirement points in the study area.

## 2.6. Future Water Security

Three key indices are commonly used to evaluate water security, namely reliability, resilience, and vulnerability (RRV). Hashimoto et al. [43] introduced the concept of the RRV in the context of water resource systems. The reliability ( $R_{el}$ ) index measures the probability that a system is in a satisfactory state and is defined as the ratio of the number of time steps where demand is met to the total number of time steps; a higher reliability indicates a more dependable water system. Resilience ( $R_{es}$ ) quantifies the ability of a system to recover from failure to a satisfactory state after falling below a satisfactory threshold. It can be defined as the ratio of the probability of transition from the unsatisfactory to the satisfactory state; a high resilience value indicates that the system can quickly return to a satisfactory state. Vulnerability ( $V_{ul}$ ) assesses the extent of deficits by measuring the severity of failures when the system fails to meet demand; a lower vulnerability demonstrates less severe consequences from the failure of the system. These three indices were calculated as follows:

$$R_{el} = 1 - \frac{\sum_{j=1}^M d(j)}{T} \quad (6)$$

$$R_{es} = \left\{ \frac{1}{M} \sum_{j=1}^M d(j) \right\}^{-1} \quad (7)$$

$$V_{ul} = \frac{1}{M} \sum_{j=1}^M v(j) \quad (8)$$

where  $M$  is the total number of water deficit events,  $T$  is the number of time intervals,  $d(j)$  is the duration of the water deficit event  $j$  (days), and  $v(j)$  is the severity of the water deficit ( $\text{Mm}^3$ ).

Although individual metrics of the RRV can provide important information regarding water security, relying solely on these separate indicators may not be sufficient to analyze multiple scenarios and find solutions within them. The aggregation index ( $AI$ ) integrates these indices into a simple comprehensive score, providing a clearer evaluation of the overall state. Therefore, in this study, we applied both RRV and  $AI$  to examine future water security. The  $AI$  is estimated based on the dimensionless vulnerability ( $V_{ul.d}$ ) and is calculated as follows:

$$V_{ul.d} = \frac{\frac{1}{M} \sum_{j=1}^M v(j)}{\text{Annual demand}} \quad (9)$$

$$AI = [R_{es} \times R_{el} \times (1 - V_{ul.d})]^{1/3} \quad (10)$$

## 3. Results and Discussion

### 3.1. Calibration Results

The streamflow was calibrated using SWAT across six calibration points within the target watersheds: Jhwapo-gyo, Unam-gyo, Hyeonpo-ro, Hapgang-gyo, Yongseo-gyo, and Daeseok-gyo. Among various parameters available in SWAT, six parameters (CN2, CH\_N(2), ESCO, GW\_DELAY, and GWQMN) were adjusted for calibration (Table S3), and the calibration period spanned from 2013 to 2023. Figure 8 shows the comparison between observed and simulated streamflow. The preliminary  $R^2$  values of the calibration points ranged from approximately 0.62 to 0.81, suggesting a good to very good fit between them. Similarly, PBIAS values ranged from  $-3.31\%$  to  $+3.05\%$ , indicating proper bias in the model simulations (Table 1). Furthermore, the temporal patterns of the simulated data agreed reasonably with the observed data at all calibration points, implying that the seasonal variations and hydrological events were captured during the simulation.

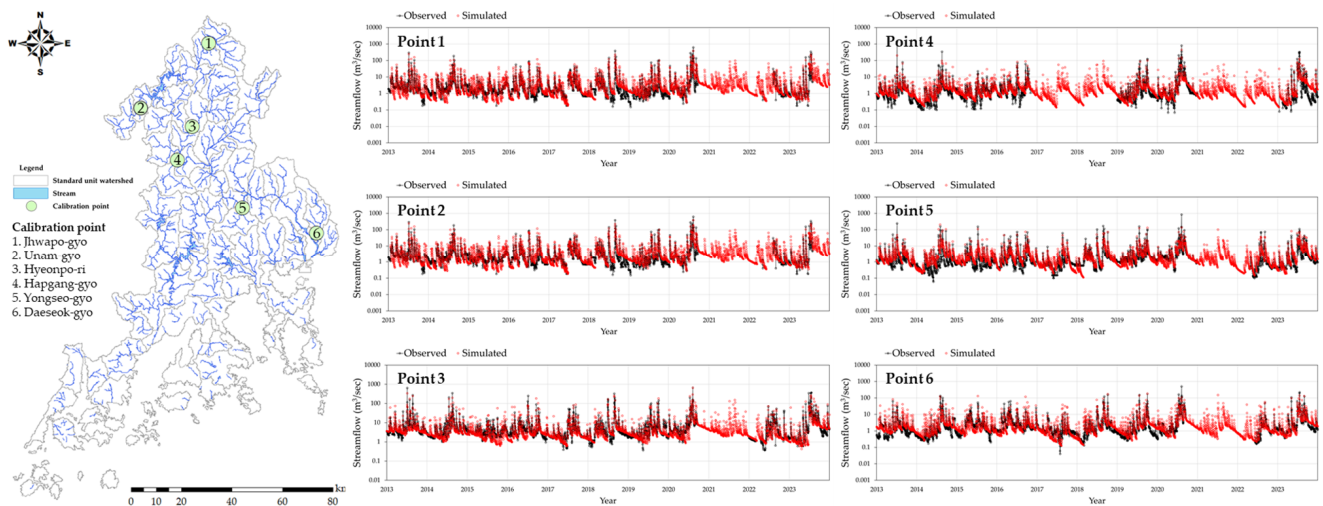


**Figure 8.** Streamflow calibration results against six calibration points. The black graph represents the observed data and the red graph represents the simulated data.

**Table 1.** Results of statistical tests during calibration of six points.

Calibration Point	R <sup>2</sup>	Percent BIAS (%)
Point 1	0.81	+2.35
Point 2	0.63	+2.90
Point 3	0.78	−0.08
Point 4	0.65	−3.31
Point 5	0.64	+3.05
Point 6	0.62	+0.86

### 3.2. Determination of Dry Scenarios

Fifteen GCMs under four different SSP scenarios were evaluated using extreme precipitation indices of the ETCCDI to derive magnitudes of dryness individually, and the results were ranked based on these indices to compare their effectiveness in representing dry scenarios in the study area. Figure 9 illustrates the dryness ranking of the 60 climate models. The sum of the scores indicates the overall performance, with lower scores representing better performance under dry scenarios. The INM-CM4-8 model under the SSP585 and SSP245 scenarios exhibited the driest performance, with total scores of 129 and 133, respectively. These results explain the superior capability of the models in simulating dry conditions, making them highly reliable for dry-scenario applications. Additionally, the MIROC6 model under SSP370 ranked among the top three models, with a score of 137, further demonstrating its proficiency in depicting dry climates.

The dryness scores for the 60 climate models ranged from 129 to 606. Although three representative models were chosen for dry scenarios, an additional model was selected to leverage the dry scenarios effectively. Models with scores of 314 or 315, which can be considered to have a moderate climate, included CNRM-ESM2-1 ssp370, MPI-ESM1-2-HR ssp585, and MRI-ESM2-0 ssp370. Given that the extreme precipitation indices of MRI-ESM2-0 ssp370 were not generally dry and showed no red areas on the heat map, MRI-ESM2-0 ssp370 was selected as a representative model for moderate climates.

The selected dry and moderate climate models were considered for SWAT to simulate unregulated flow in the future, and the flow data were input to K-WEAP to evaluate the water budget analysis and water security in the future, especially for dry and moderate climate conditions.

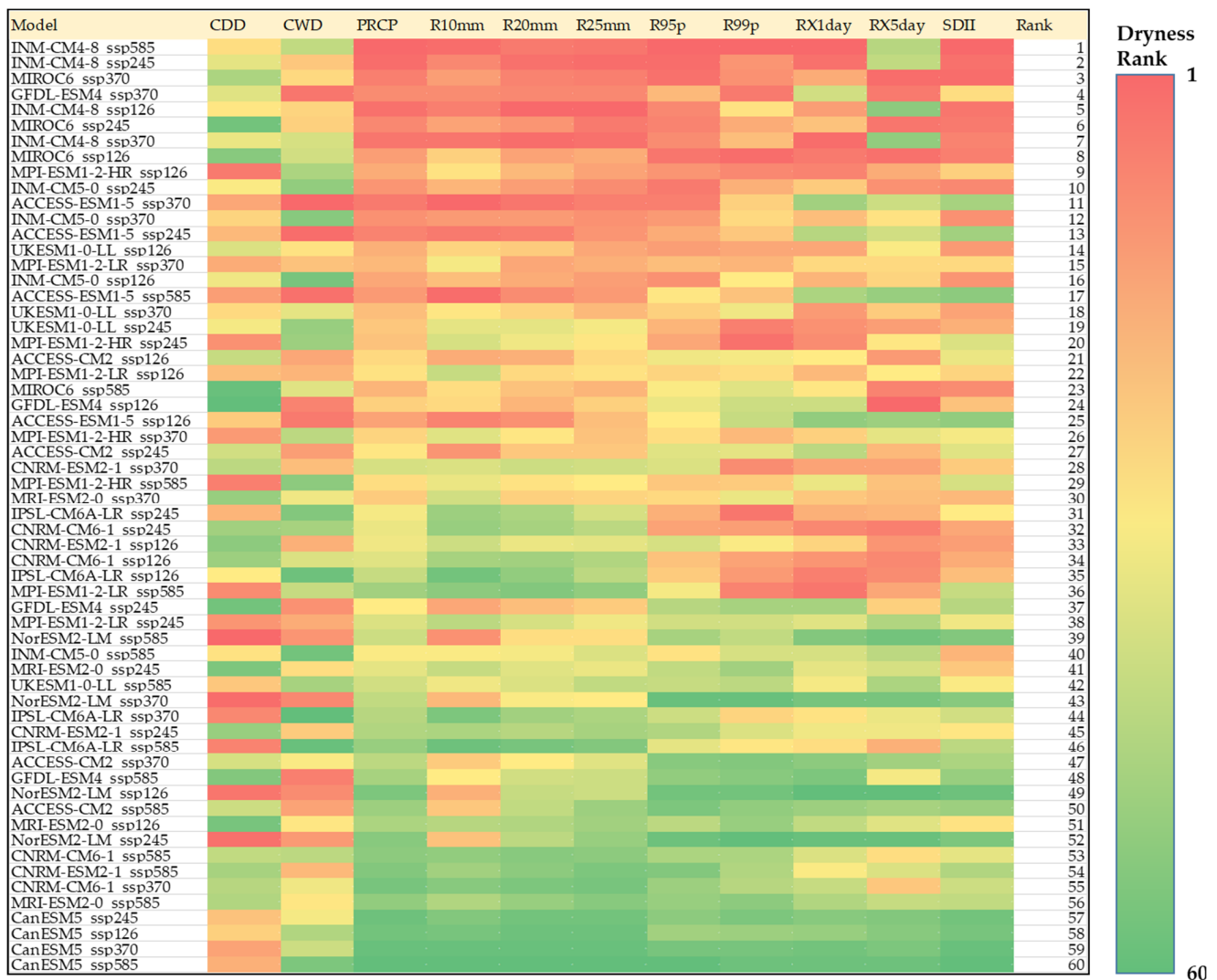


Figure 9. The 60 climate models ranked for dryness based on extreme precipitation indices.

### 3.3. Evaluation of Future Water Security

#### 3.3.1. Unmet Demand/Demand Coverage

A basic approach was used for examining water security; unmet demand and demand coverage were estimated using four climate models with five different water allocation scenarios. Table 2 presents the average values of the unmet water demand and demand coverage in the study area. INM-CM4-8 under SSP5 showed unmet demand ranging from 93.904 Mm<sup>3</sup>/year (Scenario 2) to 111.313 Mm<sup>3</sup>/year (Scenario 4), with demand coverage between 90.60% and 92.08%. For INM-CM4-8 under SSP2, unmet demand varied from 76.264 Mm<sup>3</sup>/year (Scenario 2) to 103.202 Mm<sup>3</sup>/year (Scenario 4), while demand coverage spanned from 91.97% to 93.56%. For the MIROC6 under SSP3, unmet demand was between 75.727 Mm<sup>3</sup>/year (Scenario 3) and 92.331 Mm<sup>3</sup>/year (Scenario 4), with demand coverage ranging from 92.20% to 93.60%. The model MRI-ESM2-0 under SSP3 representing a moderate scenario presented better outcomes, with unmet demand from 29.660 Mm<sup>3</sup>/year (Scenario 3) to 44.111 Mm<sup>3</sup>/year (Scenario 4) and demand coverage from 96.27% to 97.08%. Unmet demand peaked under Scenario 4 regardless of climatic conditions, whereas Scenarios 2 and 3 exhibited the lowest deficit. In contrast, the INM-CM4-8 SSP5 scenario showed the driest conditions with the worst water deficit, and this model was used as a representative dry scenario for further analysis.

**Table 2.** Results of unmet demand and demand coverage analyses for three water use types.

Climate Model	SSP	Category	Water Allocation	Unmet Demand (Mm <sup>3</sup> /year) (Demand Coverage)			
				Total	Domestic	Industrial	Agricultural
INM-CM4-8	SSP5		Scenario 1	102.155 (91.37%)	1.066 (99.10%)	28.107 (91.80%)	72.982 (89.90%)
			Scenario 2	93.904 (92.07%)	0.929 (99.22%)	19.849 (94.21%)	73.126 (89.88%)
			Scenario 3	95.074 (91.97%)	1.721 (98.55%)	20.776 (93.94%)	72.577 (89.95%)
			Scenario 4	111.313 (90.60%)	4.970 (95.82%)	32.669 (90.47%)	73.674 (89.80%)
			Scenario 5	103.842 (91.23%)	5.047 (95.75%)	25.070 (92.69%)	73.725 (89.80%)
INM-CM4-8	SSP2	Dry	Scenario 1	93.809 (92.08%)	0.718 (99.40%)	27.392 (92.01%)	65.699 (90.91%)
			Scenario 2	84.850 (92.83%)	0.599 (99.50%)	18.508 (94.60%)	65.743 (90.90%)
			Scenario 3	84.795 (92.84%)	1.219 (98.97%)	18.349 (94.65%)	65.227 (90.97%)
			Scenario 4	103.202 (91.28%)	4.533 (96.18%)	32.376 (90.56%)	66.293 (90.82%)
			Scenario 5	95.134 (91.97%)	4.530 (96.19%)	24.304 (92.91%)	66.300 (90.82%)
MIROC6	SSP3		Scenario 1	84.030 (92.90%)	1.079 (99.09%)	28.102 (91.80%)	54.849 (92.41%)
			Scenario 2	76.264 (93.56%)	0.970 (99.18%)	20.785 (93.94%)	54.509 (92.46%)
			Scenario 3	75.727 (93.60%)	1.488 (98.75%)	19.608 (94.28%)	54.631 (92.44%)
			Scenario 4	92.331 (92.20%)	4.515 (96.20%)	32.661 (90.47%)	55.155 (92.37%)
			Scenario 5	84.199 (92.89%)	4.538 (96.18%)	24.491 (92.86%)	55.170 (92.36%)
MRI-ESM2-0	SSP3	Moderate	Scenario 1	43.188 (96.35%)	0.069 (99.94%)	19.393 (94.34%)	23.726 (96.72%)
			Scenario 2	33.258 (97.19%)	0.063 (99.95%)	9.460 (97.24%)	23.735 (96.71%)
			Scenario 3	29.600 (97.50%)	0.122 (99.90%)	5.842 (98.30%)	23.636 (96.73%)
			Scenario 4	44.111 (96.27%)	0.652 (99.45%)	19.724 (94.25%)	23.735 (96.71%)
			Scenario 5	34.562 (97.08%)	0.601 (99.49%)	10.254 (97.01%)	23.707 (96.72%)

Table 2 presents the overall water deficit in the study area; however, the demand coverage was spatially distributed along the study area, and specific regions or points vulnerable to water security were identified. Figures 10–12 illustrate the average demand coverage for domestic, industrial, and agricultural water uses by administrative district or standard watershed unit. For domestic and industrial waters, water deficits are generally not severe under moderate climatic conditions. However, administrative districts within watershed 41 experienced an increase in unmet demand when water allocation shifted from domestic and industrial use to instream flow. This occurred because of the concentration of instream flow points in watershed 40 and the limited water transfer from watersheds 40 to 41 under water allocation conditions. In addition, Namwon City, located in the upper-right part of the study area, showed considerable variation in domestic water use. The city relies on water supply from the Donghwa Dam, as it has two primary sources: direct water supply from the dam and intake from the weir below the dam. However, besides its original purpose to supply agricultural water downstream, the dam provides water to five administrative districts, including Namwon City. Therefore, the limited water supply from dams in a dry climate and the prioritization of instream flow made the city susceptible to water deficits. In contrast, the demand coverage of agricultural water use showed minimal spatial variation despite the changes in water allocation, indicating that the allocation adjustments do not significantly damage agricultural water in the study area. Moreover, the results suggest that systemic factors such as the operating rules of agricultural facilities, water resource management, and irrigation systems have a greater impact than water allocation on future water security.

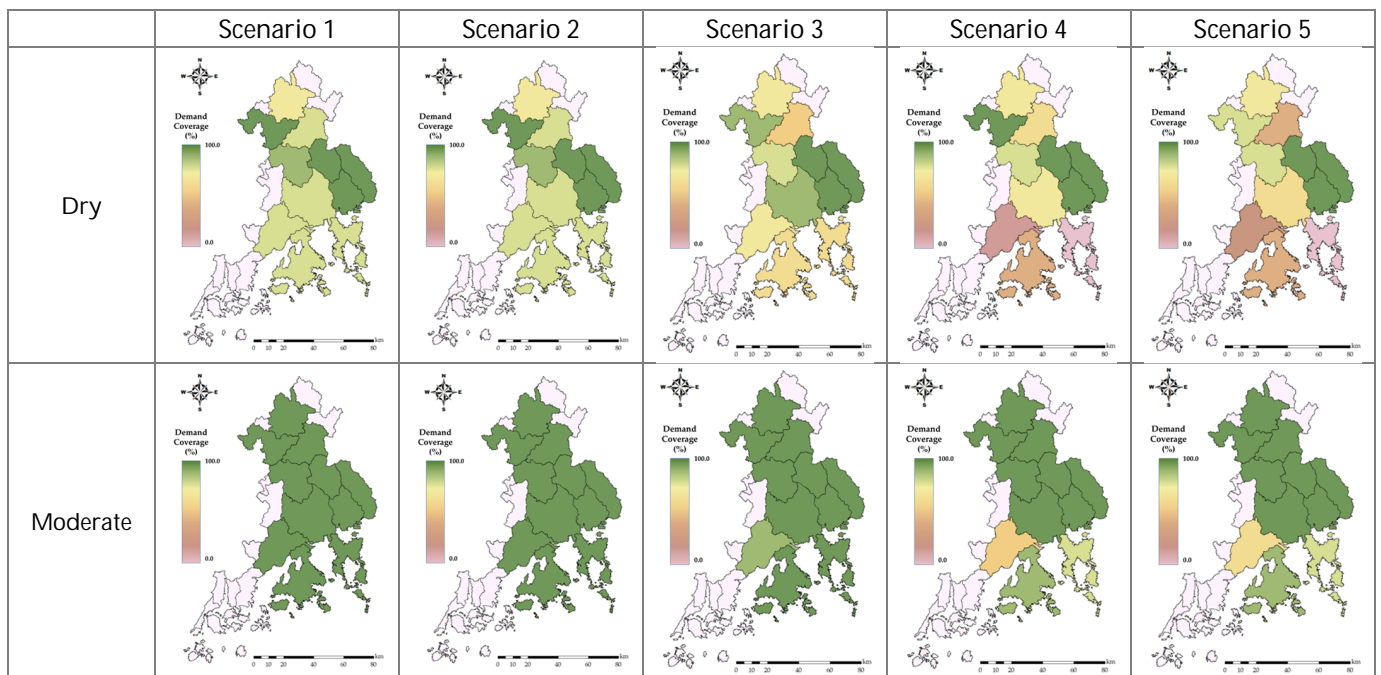


Figure 10. Demand coverage distribution for domestic water use.

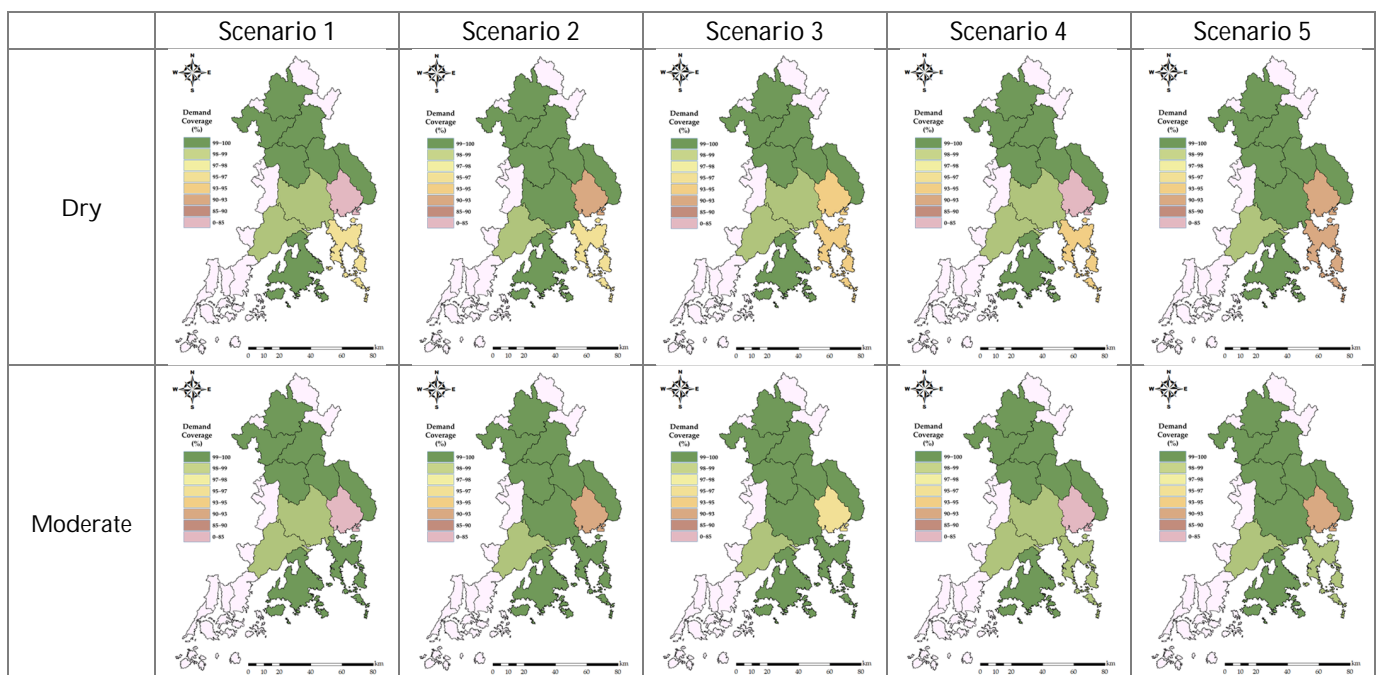


Figure 11. Demand coverage distribution for industrial water use.

Considering the climatic conditions and water allocation scenarios, the total unmet demand and demand coverage were estimated for 13 designated instream flow points. Table 3 shows the total unmet demand of the instream flow in the study area and a comparison of the variations in the three points with high unmet demand. Averaging all water allocation scenarios, the unmet instream flow under dry scenarios was 5.429 Mm<sup>3</sup>/year, whereas the performance was better under moderate scenarios, with an average value of 1.106 Mm<sup>3</sup>/year. Under moderate climate conditions, most deficits occurred at Point C, whereas they varied across different points under dry climate conditions. Under dry scenarios, Scenario 1 showed the highest unmet demand of 6.616 Mm<sup>3</sup>/year; its demand

coverage varied from 90.54% at Point C to 98.82% at Point L. The situation was slightly improved under Scenario 2 with an unmet demand of 6.508 Mm<sup>3</sup>/year and a similar coverage variability to that of Scenario 1. Unmet demand substantially reduced to 5.775 Mm<sup>3</sup>/year under Scenario 3, with a better overall coverage from 90.15% at Point C to 99.42% at Point L. Under Scenarios 4 and 5, the unmet demand further reduced to 4.616 Mm<sup>3</sup>/year and 4.629 Mm<sup>3</sup>/year, respectively, with Scenario 5 achieving a nearly perfect demand coverage of 99.99% at Point L. Regarding variations at individual points, Point C is believed to be vulnerable owing to the absence of upstream hydraulic structures and its dependence on natural runoff. Point G was located downstream of the Donghwa Dam and its limited water resources prompted vulnerability. Finally, Point L, most downstream among the instream flow points of the study area, served as a benchmark for the total runoff in the study area; its unmet demand was lower than those of other vulnerable points, thus posing no significant issues.

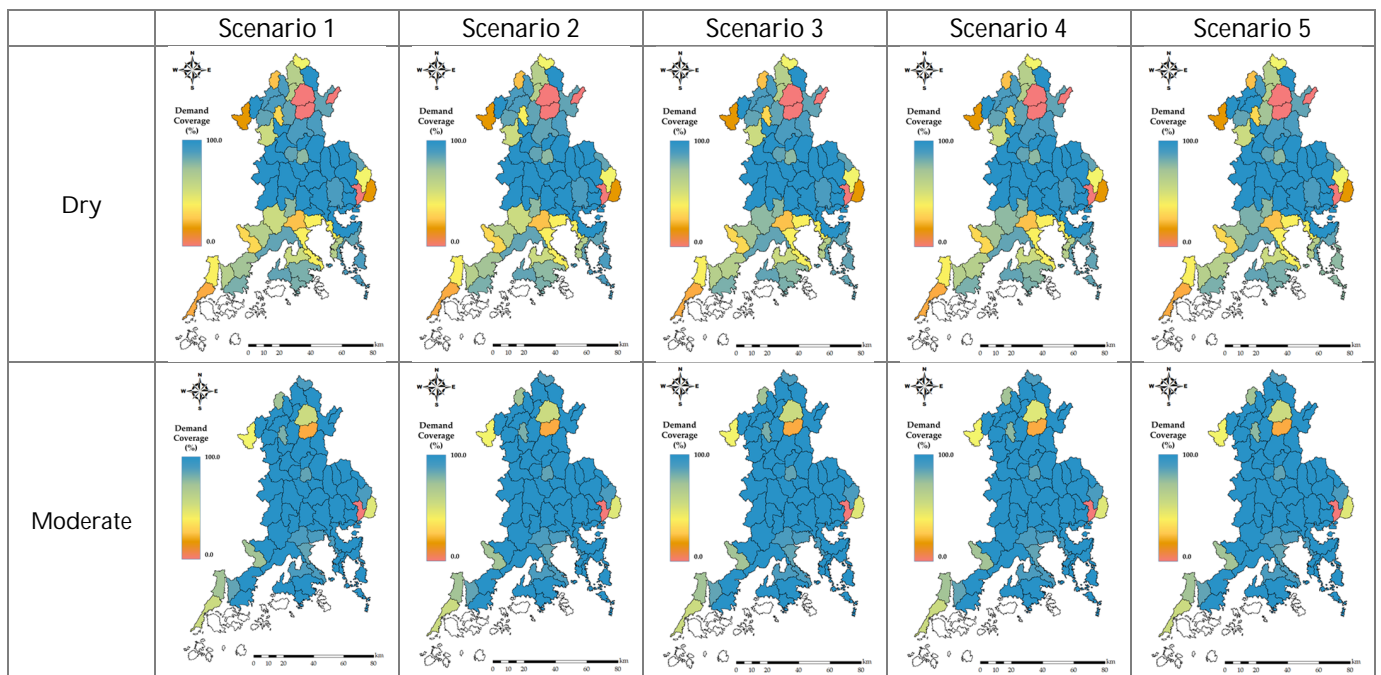


Figure 12. Demand coverage distribution for agricultural water use.

Table 3. Results of unmet demand and demand coverage analyses for instream flow.

Category	Water Allocation	Unmet Demand (Mm <sup>3</sup> /year) (Demand Coverage)			
		Total	Point C	Point G	Point L
Dry	Scenario 1	6.616	4.267 (90.54%)	1.078 (96.40%)	0.383 (98.82%)
	Scenario 2	6.508	4.262 (90.55%)	1.057 (96.47%)	0.377 (98.84%)
	Scenario 3	5.775	4.441 (90.15%)	0.688 (97.70%)	0.189 (99.42%)
	Scenario 4	4.616	3.752 (91.68%)	0.721 (97.59%)	-
	Scenario 5	4.629	3.761 (91.66%)	0.714 (97.62%)	0.008 (99.99%)
Moderate	Scenario 1	1.072	1.052 (97.67%)	-	-
	Scenario 2	1.074	1.052 (97.67%)	-	-
	Scenario 3	1.171	1.170 (97.41%)	-	-
	Scenario 4	0.958	0.958 (97.88%)	-	-
	Scenario 5	0.958	0.958 (97.88%)	-	-

### 3.3.2. RRV and AI

RRV indices were estimated for the three water uses and instream flows under various climate and water allocation conditions (Table 4). Under dry conditions, the reliability index for domestic use ranged from 0.886 to 0.956, resilience index from 0.176 to 0.316, and vulnerability index from 0.092 Mm<sup>3</sup> to 0.345 Mm<sup>3</sup>, with Scenario 4 having the lowest reliability and highest vulnerability. For industrial use, the reliability index ranged between 0.944 and 0.961, resilience index between 0.412 and 0.510, and vulnerability index between 1.097 Mm<sup>3</sup> and 1.542 Mm<sup>3</sup>, with Scenario 2 showing the best performance. Agricultural use demonstrated high reliability (0.967 to 0.968) but low resilience (0.297) and high vulnerability (1.501 Mm<sup>3</sup> to 1.542 Mm<sup>3</sup>), with minimal variation across scenarios. For instream flow, the reliability index ranged from 0.966 to 0.977, resilience index from 0.275 to 0.289, and vulnerability index from 0.720 Mm<sup>3</sup> to 0.782 Mm<sup>3</sup>, with Scenario 3 having the lowest resilience. Under moderate conditions, domestic use reliability improved significantly, ranging from 0.958 to 0.997, resilience from 0.223 to 0.588, and vulnerability from 0.020 Mm<sup>3</sup> to 0.092 Mm<sup>3</sup>, with Scenario 2 performing the best. Similarly, industrial use reliability increased to range between 0.957 and 0.972, resilience between 0.511 and 0.620, and vulnerability between 0.424 Mm<sup>3</sup> to 1.098 Mm<sup>3</sup>, showing marked improvement in Scenario 3. Agricultural use reliability index ranged from 0.967 to 0.987, with resilience index at 0.423, and vulnerability index between 0.834 Mm<sup>3</sup> and 0.852 Mm<sup>3</sup>. Instream flow reliability index ranged from 0.991 to 0.993, resilience index from 0.338 to 0.385, and vulnerability index from 0.339 Mm<sup>3</sup> to 0.415 Mm<sup>3</sup>, with the highest resilience exhibited under Scenario 2. Generally, Scenarios 2 and 3 outperformed the other scenarios in terms of reliability. However, Scenario 3 was weak in recovering from water deficit and vulnerability, which were even worse than those of Scenario 1. On prioritizing instream flow under Scenarios 4 and 5, the flow apparently recovered; however, whether its value is higher than the loss in domestic and industrial water use needs to be accounted for.

**Table 4.** Reliability, resilience, and vulnerability indices for all water uses.

Water Use	Climate	Index	Water Allocation Scenario				
			Scenario 1	Scenario 2	Scenario 3	Scenario 4	Scenario 5
Domestic	Dry	R <sub>el</sub> (%)	0.951	0.956	0.925	0.886	0.890
		R <sub>es</sub>	0.311	0.316	0.255	0.176	0.178
		V <sub>ul</sub> (Mm <sup>3</sup> )	0.093	0.092	0.123	0.330	0.345
	Moderate	R <sub>el</sub> (%)	0.996	0.997	0.982	0.958	0.964
		R <sub>es</sub>	0.588	0.543	0.428	0.223	0.235
		V <sub>ul</sub> (Mm <sup>3</sup> )	0.030	0.048	0.020	0.092	0.092
Industrial	Dry	R <sub>el</sub> (%)	0.946	0.956	0.961	0.944	0.952
		R <sub>es</sub>	0.453	0.510	0.476	0.412	0.426
		V <sub>ul</sub> (Mm <sup>3</sup> )	1.419	1.097	1.334	1.532	1.542
	Moderate	R <sub>el</sub> (%)	0.956	0.964	0.972	0.957	0.964
		R <sub>es</sub>	0.542	0.588	0.620	0.511	0.550
		V <sub>ul</sub> (Mm <sup>3</sup> )	0.971	0.557	0.424	1.098	0.645
Agricultural	Dry	R <sub>el</sub> (%)	0.967	0.968	0.968	0.968	0.968
		R <sub>es</sub>	0.297	0.297	0.294	0.293	0.293
		V <sub>ul</sub> (Mm <sup>3</sup> )	1.501	1.510	1.500	1.532	1.542
	Moderate	R <sub>el</sub> (%)	0.987	0.987	0.987	0.987	0.987
		R <sub>es</sub>	0.423	0.423	0.424	0.423	0.423
		V <sub>ul</sub> (Mm <sup>3</sup> )	0.852	0.851	0.834	0.837	0.837



Table 4. Cont.

Water Use	Climate	Index	Water Allocation Scenario				
			Scenario 1	Scenario 2	Scenario 3	Scenario 4	Scenario 5
Instream flow	Dry	R <sub>el</sub> (%)	0.966	0.967	0.972	0.977	0.977
		R <sub>es</sub>	0.288	0.289	0.279	0.276	0.275
		V <sub>ul</sub> (Mm <sup>3</sup> )	0.732	0.720	0.782	0.777	0.779
	Moderate	R <sub>el</sub> (%)	0.991	0.991	0.992	0.993	0.993
		R <sub>es</sub>	0.384	0.385	0.359	0.338	0.338
		V <sub>ul</sub> (Mm <sup>3</sup> )	0.342	0.339	0.412	0.415	0.414

Information on possible water deficits in the study area was collected by examining the RRV indices under each scenario. However, defining the best strategy to strengthen the study area against a dry climate remains ambiguous because of multiple indices with different patterns. Therefore, the AI based on the RRV indices was estimated to determine the scenarios that were valid under dry conditions. Figure 13 presents a bar graph of the AI value for each scenario. Generally, the AI of all water uses and instream flows tended to decrease as dryness increased. Scenario 2 showed the highest AI for domestic and industrial use under dry conditions, with values of 0.671 and 0.786, respectively. Scenario 4 had the lowest index for domestic use under both dry and moderate conditions, with values of 0.537 and 0.598, respectively. Scenario 3 showed the highest index for industrial use (0.844) under moderate climatic conditions, suggesting improved water allocation. The prioritization of instream flow and deprioritization of agricultural water did not greatly influence the AI under either moderate or dry climate conditions. Therefore, domestic and industrial water uses were highly sensitive to both climate and water allocation conditions, whereas the others were not notably affected by water allocation.

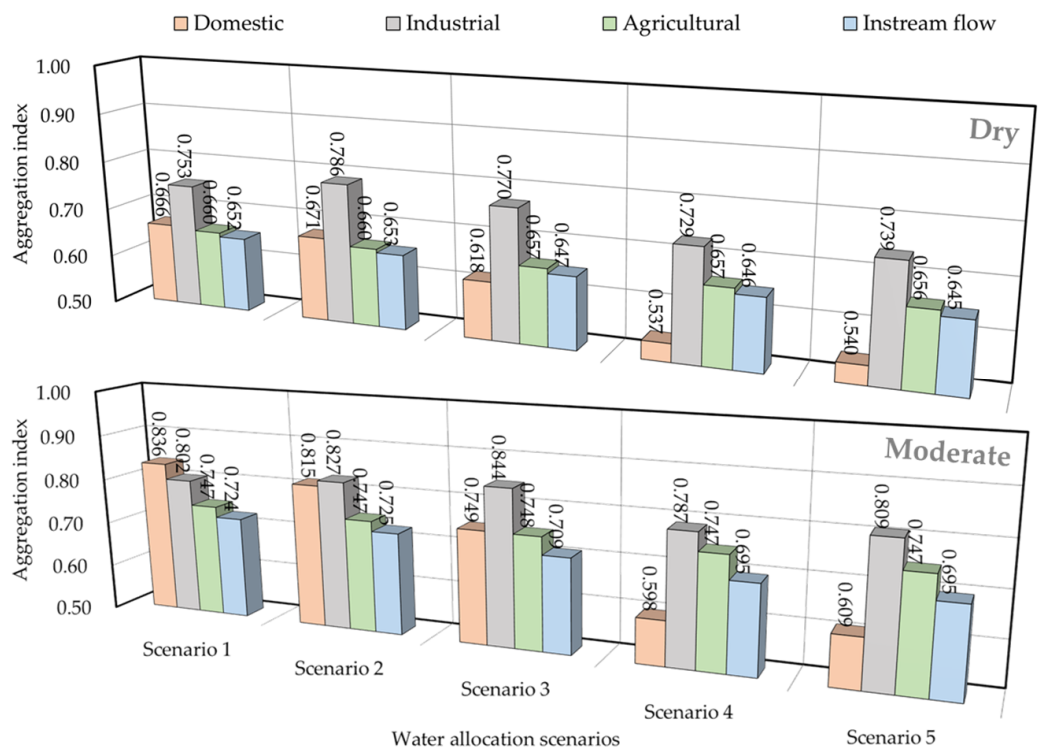


Figure 13. AIs for different water allocation scenarios under dry and moderate climatic conditions.

#### 4. Conclusions

This study conducted a water budget analysis of the Seomjin River Basin, a drought-prone watershed, by adopting practical water allocation scenarios. The allocation scenarios included priority shifting between domestic, industrial, and agricultural water uses and instream flow. The impact of water allocation changes on water security was assessed under future dry and moderate climatic conditions, which were determined from the extreme precipitation indices of the ETCCDI. The future water security was evaluated from multiple perspectives based on unmet demand, demand coverage, RRV, and AI. Variations imposed by climate conditions and water allocation changes were examined separately and comprehensively, focusing on determining the best strategy for target watersheds to mitigate future drought-related water deficits.

The water allocation system showed variability in water security under different climatic conditions, with Scenario 4 (prioritizing instream flow) having the highest unmet demand and Scenarios 2 and 3 having the lowest. Scenario 2, prioritizing domestic and industrial water, was most suitable in dry climates, whereas Scenario 3, with equal water distribution, was best for moderate climates. Although Scenarios 2 and 3 generally outperformed others in terms of reliability, Scenario 3 had issues with resilience and vulnerability. Scenarios 4 and 5 improved the instream flow reliability but at the expense of domestic and industrial water uses. Agricultural water use remained stable across scenarios owing to its reliance on reservoirs and irrigation dams. An AI based on RRV indicators highlighted that Scenario 2 consistently performed well for domestic and industrial water uses under dry conditions. This implies that domestic and industrial water uses are highly sensitive to water allocation, whereas instream flow was less affected by water allocation changes.

There are few limitations to consider. First, the scope of climate models and water allocation scenarios in this study may not fully capture the wide range of possible climate changes and regional conditions. Second, the water allocation priorities were tailored to the specific conditions of the Seomjin River Basin, making it difficult to generalize the findings to other regions or countries. Therefore, future research should incorporate a broader range of climate scenarios and water management strategies, while also considering regional characteristics and the uncertainties of climate change for more detailed and comprehensive analyses.

The findings comprehensively demonstrated that managing water allocation priorities in the Seomjin River Basin could highly influence the water resource system, and prioritizing domestic and industrial water is the most suitable strategy. The evaluation of water security varies depending on the analytical perspective, which means that there is a possibility that a flexible plan could ensure optimal water allocation. Ultimately, future water management policies should prioritize the sectors most sensitive to climate variability while meeting ecological needs without compromising human and industrial water security [44]. Therefore, water management approaches that consider multidimensional water allocation strategies must be studied further.

**Supplementary Materials:** The following supporting information can be downloaded at: <https://www.mdpi.com/article/10.3390/w16202933/s1>. Table S1. GCMs used for SWAT simulation; Table S2. Definition of extreme precipitation indices [45–57]; Table S3. Adjusted SWAT parameters.

**Author Contributions:** Conceptualization, W.K. and S.C.; methodology, W.K.; software, S.C.; validation, S.K. and S.W.; resources, S.K.; data curation, S.W.; writing—original draft preparation, W.K.; writing—review and editing, W.K. and S.C.; visualization, S.K. and S.W.; supervision, S.C.; project administration, S.C.; funding acquisition, S.C. All authors have read and agreed to the published version of the manuscript.

**Funding:** This work was supported by Korea Environment Industry and Technology Institute (KEITI) through the Water Management Program for Drought, funded by Korea Ministry of Environment (MOE) (2022003610004).

**Data Availability Statement:** Data are contained within the article.

**Conflicts of Interest:** The authors declare no conflicts of interest.

## References

1. Intergovernmental Panel on Climate Change (IPCC). *Climate Change 2014: Synthesis Report. Contribution of Working Groups I, II and III to the Fifth Assessment Report of the Intergovernmental Panel on Climate Change*; IPCC: Geneva, Switzerland, 2014; p. 151. [[CrossRef](#)]
2. Yang, D.; Zhang, H.; Wang, Z.; Zhao, S.; Li, J. Changes in anthropogenic particulate matters and resulting global climate effects since the Industrial Revolution. *Int. J. Climatol.* **2022**, *42*, 315–330. [[CrossRef](#)]
3. Intergovernmental Panel on Climate Change (IPCC). *Climate Change 2022: Impacts, Adaptation, and Vulnerability. Contribution of Working Group II to the Sixth Assessment Report of the Intergovernmental Panel on Climate Change*, 6th ed.; Pörtner, H.-O., Roberts, D.C., Poloczanska, E.S., Mintenbeck, K., Tignor, M., Alegría, A., Craig, M., Langsdorf, S., Lösschke, S., Möller, V., et al., Eds.; Cambridge University Press: Cambridge, UK; New York, NY, USA, 2022; pp. 3–33. [[CrossRef](#)]
4. ME (Ministry of the Environment). *The 1st Master Plan for National Water Management (2021–2030)*; ME (Ministry of the Environment): Sejong, Republic of Korea, 2021. (In Korean)
5. NIMS (National Institute of Meteorological Sciences). *Report on High-Resolution Projection of Future Climate Change*; NIMS (National Institute of Meteorological Sciences): Jeju-island, Republic of Korea, 2022. (In Korean)
6. Dubrovsky, M.; Svoboda, M.D.; Trnka, M.; Hayes, M.J.; Wilhite, D.A.; Zalud, Z.; Hlavinka, P. Application of relative drought indices in assessing climate-change impacts on drought conditions in Czechia. *Theor. Appl. Climatol.* **2009**, *96*, 155–171. [[CrossRef](#)]
7. Wilhite, D.A. Integrated drought management: Moving from managing disasters to managing risk. *Integr. Drought Manag.* **2024**, *2*, 507–514.
8. Lloyd-Hughes, B. The impracticality of a universal drought definition. *Theor. Appl. Climatol.* **2014**, *117*, 607–611. [[CrossRef](#)]
9. Vargas Molina, J.; Paneque Salgado, P. Methodology for the analysis of causes of drought vulnerability on river basin scale. *Nat. Hazards* **2017**, *89*, 609–621. [[CrossRef](#)]
10. Watts, G.; von Christerson, B.; Hannaford, J.; Lonsdale, K. Testing the resilience of water supply systems to long droughts. *J. Hydrol.* **2012**, *414–415*, 255–267. [[CrossRef](#)]
11. Huntington, T.G. Evidence for intensification of the global water cycle: Review and synthesis. *J. Hydrol.* **2006**, *319*, 83–95. [[CrossRef](#)]
12. Sheffield, J.; Wood, E.F. Projected changes in drought occurrence under future global warming from multi-model, multi-scenario, IPCC AR4 simulations. *Clim. Dyn.* **2008**, *31*, 79–105. [[CrossRef](#)]
13. Cayan, D.R.; Das, T.; Pierce, D.W.; Barnett, T.P.; Tyree, M.; Gershunov, A. Future dryness in the southwest US and the hydrology of the early 21st century drought. *Proc. Natl. Acad. Sci. USA* **2010**, *107*, 21271–21276. [[CrossRef](#)]
14. WWAP. *The United Nations World Water Development Report 2016: Water and Jobs*; United Nations World Water Assessment Programme; UNESCO: Paris, France, 2016.
15. Guimarães, L.T.; Magrini, A. A proposal of indicators for sustainable development in the management of river basins. *Water Resour. Manag.* **2008**, *22*, 1191–1202. [[CrossRef](#)]
16. Harmancioglu, N.B. Overview of water policy developments: Pre- and post-2015 development agenda. *Water Resour. Manag.* **2017**, *31*, 3001–3021. [[CrossRef](#)]
17. Navarro-Ramírez, V.; Ramírez-Hernandez, J.; Gil-Samaniego, M.; Eliana Rodríguez-Burgueño, J.E. Methodological frameworks to assess sustainable water resources management in industry: A review. *Ecol. Indic.* **2020**, *119*, 106819. [[CrossRef](#)]
18. OECD Publishing. *Water Resources Allocation: Sharing Risks and Opportunities*; OECD Publishing: Paris, France, 2015.
19. Lee, H.J.; Shim, M.P. Decision making for priority of water allocation during drought by analytic hierarchy process. *J. Korea Water Resour. Assoc.* **2002**, *35*, 703–714. [[CrossRef](#)]
20. Choi, S.J.; Kim, J.H.; Lee, D.R. Decision of the water shortage mitigation policy using multi-criteria decision analysis. *KSCE J. Civ. Eng.* **2012**, *16*, 247–253. [[CrossRef](#)]
21. Lim, J.S.; Kang, S.W.; Kim, H.N.; Lee, E.R. Evaluation of potential securing instream flow according to estimating operation rule in Naeseongcheon watershed. *Korean Soc. Hazard Mitig.* **2017**, *17*, 265–277. [[CrossRef](#)]
22. Kim, D.; Chun, J.A.; Choi, S.J. Incorporating the logistic regression into a decision-centric assessment of climate change impacts on a complex river system. *Hydrol. Earth Syst. Sci.* **2019**, *23*, 1145–1162. [[CrossRef](#)]
23. Wang, Z.; Zhang, L.; Cheng, L.; Liu, K.; Ye, A.; Cai, X. Optimizing operating rules for a reservoir system in northern China considering ecological flow requirements and water use priorities. *J. Water Resour. Plan. Manag.* **2020**, *146*, 04020051. [[CrossRef](#)]
24. Luo, P.; Sun, Y.; Wang, S.; Wang, S.; Lyu, J.; Zhou, M.; Nakagami, K.; Takara, K.; Nover, D. Historical assessment and future sustainability challenges of Egyptian water resources management. *J. Clean. Prod.* **2020**, *263*, 121154. [[CrossRef](#)]
25. Zehtabian, E.; Masoudi, R.; Yazdandoost, F.; Sedghi-Asl, M.; Loáiciga, H.A. Investigation of water allocation using integrated water resource management approaches in the Zayandehroud River basin, Iran. *J. Clean. Prod.* **2023**, *395*, 136339. [[CrossRef](#)]
26. Arnold, J.G.; Srinivasan, R.; Muttiah, R.S.; Williams, J.R. Large area hydrologic modeling and assessment part I: Model development 1. *J. Am. Water Resour. Assoc.* **1998**, *34*, 73–89. [[CrossRef](#)]
27. Arnold, J.G.; Moriasi, D.N.; Gassman, P.W.; Abbaspour, K.C.; White, M.J.; Srinivasan, R.; Santhi, R.D.; Harmel, A.; van Griensven, M.W.; Van Liew, N.; et al. SWAT: Model use, calibration, and validation. *Trans. ASABE* **2012**, *55*, 1491–1508. [[CrossRef](#)]

28. Gassman, P.W.; Reyes, M.R.; Green, C.H.; Arnold, J.G. The soil and water assessment tool: Historical development, applications, and future research directions. *Trans. ASABE* **2007**, *50*, 1211–1250. [[CrossRef](#)]
29. Neitsch, S.L.; Arnold, J.G.; Kiniry, J.R.; Williams, J.R. *Soil and Water Assessment Tool Theoretical Documentation Version 2009*; Texas Water Resources Institute: College Station, TX, USA, 2011.
30. Krysanova, V.; White, M. Advances in water resources assessment with SWAT—An overview. *Hydrol. Sci. J.* **2015**, *60*, 1–13. [[CrossRef](#)]
31. Choi, S.J.; Lee, D.R.; Moon, J.W.; Kang, S.K. Application of K-WEAP (Korea-integrated water resources evaluation and planning model). *J. Korea Water Resour. Assoc.* **2010**, *43*, 625–633. [[CrossRef](#)]
32. Kang, S.K.; Choi, S.J.; Lee, D.R. Evaluation and re-estimation of instream flow considering the water quality and aquatic ecosystem of the Seomjingang River watershed. *J. Korean Soc. Hazard Mitig.* **2021**, *21*, 347–355. [[CrossRef](#)]
33. Jeong, G.; Kang, D. Hydro-Economic Water Allocation model for water supply risk analysis: A case study of Namhan River Basin, South Korea. *Sustainability* **2021**, *13*, 6005. [[CrossRef](#)]
34. Kim, Y.J.; Wu, D.; Lee, J.H.; Kim, J.S.; Park, S.Y. Evaluation and securing of ecological flow by linking fish growth scenarios and basin water budget analysis. *Ecol. Indic.* **2024**, *158*, 111468. [[CrossRef](#)]
35. Ministry of Land, Infrastructure and Transport. *The 4th Long-Term Comprehensive Plan of Water Resources 2001–2020*, 3rd ed.; K-Water; MOLIT: Seoul, Republic of Korea, 2016. (In Korean)
36. Huang, Q.; Ju, W.; Zhang, F.; Zhang, Q. Roles of climate change and increasing CO<sub>2</sub> in driving changes of net primary productivity in China simulated using a dynamic global vegetation model. *Sustainability* **2019**, *11*, 4176. [[CrossRef](#)]
37. Eyring, V.; Bony, S.; Meehl, G.A.; Senior, C.A.; Stevens, B.; Stouffer, R.J.; Taylor, K.E. Overview of the Coupled Model Intercomparison Project Phase 6 (CMIP6) experimental design and organization. *Geosci. Model Dev.* **2016**, *9*, 1937–1958. [[CrossRef](#)]
38. Simpkins, G. Progress in climate modelling. *Nat. Clim. Change* **2017**, *7*, 684–685. [[CrossRef](#)]
39. Zhang, X.; Alexander, L.; Hegerl, G.C.; Jones, P.; Tank, A.K.; Peterson, T.C.; Trewin, B.; Zwiers, F.W. Indices for monitoring changes in extremes based on daily temperature and precipitation data. *Wiley Interdiscip. Rev. Clim. Change* **2011**, *2*, 851–870. [[CrossRef](#)]
40. Estrela, T.; Vargas, E. Drought management plans in the European Union. The case of Spain. *Water Resour. Manag.* **2012**, *26*, 1537–1553. [[CrossRef](#)]
41. Capra, A.; Consoli, S.; Scicolone, B. Long-term climatic variability in Calabria and effects on drought and agrometeorological parameters. *Water Resour. Manag.* **2013**, *27*, 601–617. [[CrossRef](#)]
42. Lee, J.J.; Kwon, H.H.; Kim, T.W. Spatio-temporal analysis of extreme precipitation regimes across South Korea and its application to regionalization. *J. Hydro-Environ. Res.* **2012**, *6*, 101–110. [[CrossRef](#)]
43. Hashimoto, T.; Stedinger, J.R.; Loucks, D.P. Reliability, resiliency, and vulnerability criteria for water resource system performance evaluation. *Water Resour. Res.* **1982**, *18*, 14–20. [[CrossRef](#)]
44. Varady, R.G.; Zuniga-Teran, A.A.; Garfin, G.M.; Martín, F.; Vicuña, S. Adaptive management and water security in a global context: Definitions, concepts, and examples. *Curr. Opin. Environ. Sustain.* **2016**, *21*, 70–77. [[CrossRef](#)]
45. Bi, D.; Dix, M.; Marsland, S.; O’Farrell, S.; Sullivan, A.; Bodman, R.; Law, R.; Harman, I.; Srbinovsky, J.; Rashid, H.A.; et al. Configuration and spin-up of ACCESS-CM2, the new generation Australian Community Climate and Earth System Simulator Coupled Model. *J. South. Hemisph. Earth Syst. Sci.* **2020**, *70*, 225–251. [[CrossRef](#)]
46. Swart, N.C.; Cole, J.N.S.; Kharin, V.V.; Lazare, M.; Scinocca, J.F.; Gillett, N.P.; Anstey, J.; Arora, V.; Christian, J.R.; Jiao, Y. *CCCma CanESM5 Model Output Prepared for CMIP6 ScenarioMIP*; Earth System Grid Federation: Washington, DC, USA, 2019.
47. Voldoire, A. *CNRM-CERFACS CNRM-CM6-1 Model Output Prepared for CMIP6 ScenarioMIP*; Earth System Grid Federation: Washington, DC, USA, 2019.
48. John, J.G.; Blanton, C.; McHugh, C.; Radhakrishnan, A.; Rand, K.; Vahlenkamp, H.; Wilson, C.; Zadeh, N.T.; Dunne, J.P.; Dussin, R.; et al. *NOAA-GFDL GFDL-ESM4 Model Output Prepared for CMIP6 ScenarioMIP*; Earth System Grid Federation: Washington, DC, USA, 2018.
49. Volodin, E.; Mortikov, E.; Gritsun, A.; Lykossov, V.; Galin, V.; Diansky, N.; Gusev, A.; Kostykin, S.; Iakovlev, N.; Shestakova, A.; et al. *INM INM-CM4-8 Model Output Prepared for CMIP6 ScenarioMIP*; Earth System Grid Federation: Washington, DC, USA, 2019.
50. Volodin, E.; Mortikov, E.; Gritsun, A.; Lykossov, V.; Galin, V.; Diansky, N.; Gusev, A.; Kostykin, S.; Iakovlev, N.; Shestakova, A.; et al. *INM INM-CM5-0 Model Output Prepared for CMIP6 ScenarioMIP ssp370*; Earth System Grid Federation: Washington, DC, USA, 2019.
51. Boucher, O.; Denvil, S.; Levvasseur, G.; Cozic, A.; Caubel, A.; Foujols, M.A.; Meurdesoif, Y.; Cadule, P.; Devilliers, M.; Dupont, E.; et al. *IPSL IPSL-CM6A-LR Model Output Prepared for CMIP6 ScenarioMIP*; Earth System Grid Federation: Washington, DC, USA, 2019.
52. Tatebe, H.; Ogura, T.; Nitta, T.; Komuro, Y.; Ogochi, K.; Takemura, T.; Sudo, K.; Sekiguchi, M.; Abe, M.; Saito, F.; et al. Description and basic evaluation of simulated mean state, internal variability, and climate sensitivity in MIROC6. *Geosci. Model Dev.* **2019**, *12*, 2727–2765. [[CrossRef](#)]
53. Mauritsen, T.; Bader, J.; Becker, T.; Behrens, J.; Bittner, M.; Brokopf, R.; Brovkin, V.; Claussen, M.; Crueger, T.; Esch, M.; et al. Developments in the MPI-M Earth System Model version 1.2 (MPI-ESM1.2) and Its Response to Increasing CO<sub>2</sub>. *J. Adv. Model. Earth Syst.* **2019**, *11*, 998–1038. [[CrossRef](#)]

54. Wieners, K.H.; Giorgetta, M.; Jungclaus, J.; Reick, C.; Esch, M.; Bittner, M.; Gayler, V.; Haak, H.; de Vrese, P.; Raddatz, T.; et al. *MPI-M MPIESM1.2-LR Model Output Prepared for CMIP6 ScenarioMIP*; Earth System Grid Federation: Washington, DC, USA, 2019. [[CrossRef](#)]
55. Yukimoto, S.; Koshiro, T.; Kawai, H.; Oshima, N.; Yoshida, K.; Urakawa, S.; Tsujino, H.; Deushi, M.; Tanaka, T.; Hosaka, M.; et al. *MRI MRI-ESM2.0 Model Output Prepared for CMIP6 ScenarioMIP*; Earth System Grid Federation: Washington, DC, USA, 2019.
56. Seland, Ø.; Bentsen, M.; Olivié, D.; Toniazzo, T.; Gjermundsen, A.; Graff, L.S.; Debernard, J.B.; Gupta, A.K.; He, Y.C.; Kirkevåg, A.; et al. Overview of the Norwegian Earth System Model (NorESM2) and key climate response of CMIP6 DECK, historical, and scenario simulations. *Geosci. Model Dev.* **2020**, *13*, 6165–6200. [[CrossRef](#)]
57. Good, P.; Sellar, A.; Tang, Y.; Rumbold, S.; Ellis, R.; Kelley, D.; Kuhlbrodt, T.; Walton, J.; Ukesm, M. *1.0-LL Model Output Prepared for CMIP6 ScenarioMIP*; Earth System Grid Federation: Washington, DC, USA, 2019.

**Disclaimer/Publisher’s Note:** The statements, opinions and data contained in all publications are solely those of the individual author(s) and contributor(s) and not of MDPI and/or the editor(s). MDPI and/or the editor(s) disclaim responsibility for any injury to people or property resulting from any ideas, methods, instructions or products referred to in the content.